J|A|C|S COMMUNICATIONS

Published on Web 10/20/2009

Heating and Cooling Dynamics of Carbon Nanotubes Observed by Temperature-Jump Spectroscopy and Electron Microscopy

Omar F. Mohammed, Peter C. Samartzis, and Ahmed H. Zewail*

Physical Biology Center for Ultrafast Science and Technology, Arthur Amos Noyes Laboratory of Chemical Physics, California Institute of Technology, Pasadena, California 91125

Received September 23, 2009; E-mail: zewail@caltech.edu

Since their discovery,[1] carbon nanotubes (CNTs) have been the subject of numerous studies, including applications in biotechnology and cell therapy.[2,3] One important characteristic of CNTs is their ability to efficiently convert light into thermal energy. Through vibrational excitations (phonons), the temperature rise can reach thousands of degrees.[4,5] Remarkably, at such high temperatures, up to 4000 K,[5] the nanotubes exhibit exceptional thermal stability and robustness when compared with, e.g., graphite or even diamond. Although thermal effects of suspended CNTs in solution have extensively been studied[6,7] (by examining the time scale of bubble formation as a result of heat transfer from the hot nanotubes to the solvent), what remain unclear are the primary steps involved in the heating of the tubes and the cooling to the surrounding medium.

In this communication, we report real-time observation of the dynamics of CNTs following infrared (IR) ultrafast excitation. Two techniques are invoked. The first is the ultrafast *T*-jump probing, which provides the time scales involved in CNTs heating and cooling. For this approach, carboxyl-functionalized CNTs were utilized to map heat rise/decay by monitoring the spectral change with time. The high solubility of the functionalized CNTs is essential for the investigation reported here, as it enables studies in different polar solvents. The second approach is direct imaging in our ultrafast electron microscope, with *in situ* infrared irradiation. The images provide the evidence for the heat transfer from the CNTs to the environment and the spatial extent of the heat wave following the irradiation.

Figure 1A displays the UV-to-IR absorption (red) and the fluoresence spectra (green) of the carboxyl-functionalized multi-walled carbon nanotubes (MWNTs) in water. The fluorescence spectrum of the functionalized tubes in the visible range has been attributed to the trapping of excitation energy by defect sites, which are generated in the nanotube structure during the acidic oxidation of the raw samples.[8−10] Steady-state fluorescence measurements at different temperatures show a decrease of fluorescence with increasing temperature. However, in these studies it is difficult to quantitatively assign a specific temperature increase to the percentage change of fluorescence, because during the long acquisition time CNTs sedimentation occurs, altering the concentration in the solution and resulting in large statistical errors in repeated fluorescence measurements.

In the ultrafast *T*-jump studies reported here, an infrared laser pulse at 1400 nm is used to heat the nanotubes followed by a UV laser pulse at 280 nm (<1 nJ/pulse) which induces CNTs fluorescence.[11,12] By monitoring the fluorescence as a function of the delay time between the heating and probing pulses, we obtained the transients shown in Figure 1B for water and methanol (MeOH) and similarly for dimethyl formamide (DMF). The heating, reflected in the fluorescence change, takes place in 16 ps for water and 35 ps for MeOH; for DMF (not shown) it is ∼30 ps. The observed difference in heating rates can be attributed to a different conformation of the nanotube bundles in each solvent. In CNTs heating involves carrier excitation, which is converted to heat by the electron−phonon coupling, and different bundle conformations can thus affect the rate of transfer. When these experiments were repeated at a higher initial temperature (70 °C), the observed time constants were not significantly altered, suggesting that the fluorescence change is due to nanotube excitation, as confirmed below. On the time scale of CNTs heating, the solvent remains "cold", as DMF and MeOH do not absorb at the excitation wavelength, and for water, heating is negligible because of the low laser power (700 nJ/pulse) used; for comparison, a typical *T*-jump experiment involving water heating with tryptophan as a fluores-

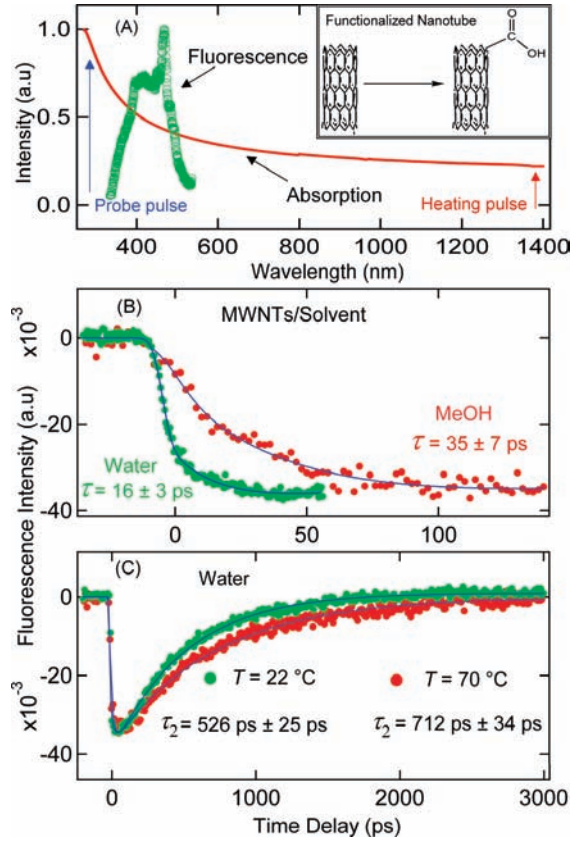

Figure 1. Transient evolution following ultrafast *T*-jump. (A) Normalized UV-to-IR absorption (red), corrected for solvent bands, and the fluoresence spectra (green) in water upon excitation at 280 nm. Inset shows schematic representation of carboxyl-functionalization of the nanotube. (B) Time dependence of the fluorescence change of MWNTs in MeOH and water following IR excitation (1.40 μm, 400−700 nJ/pulse) at 22 °C initial temperature. (C) Fluorescence change (heating) and recovery (cooling) in H_2O at 22 °C (green) and 70 °C (red) initial temperatures. The fluorescence was monitored between 310 to 550 nm. The range of concentration of the CNTs was 0.5−0.8 mg/2 mL. The solid curves are the best fits.

10.1021/ja908079x CCC: $40.75

cence indicator requires laser powers of 25−30 μJ/pulse to increase the temperature by 12 °C.[12] An estimate of the temperature at equilibrium made from knowledge of the heat capacity[13] and the average dimensions of the tubes (15 nm diameter × 1 μm length) gives, for the pulse energy of 500 nJ, a temperature in the range of 1000−5000 K.

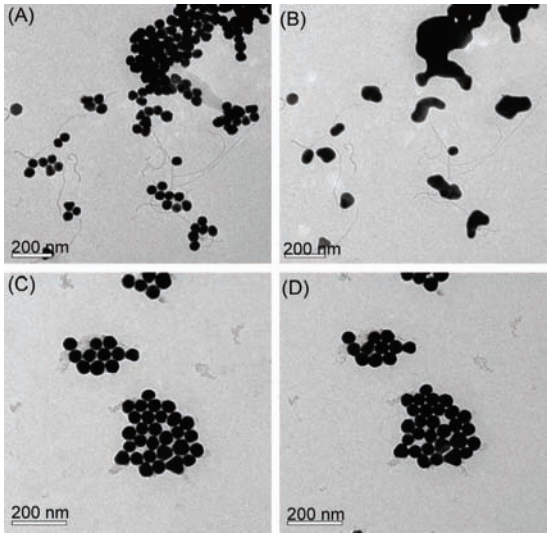

Figure 2. Electron micrographs of gold nanoparticles with and without MWNTs, taken before and after 776 nm *in situ* pulsed laser irradiation. In the specimen containing the nanotubes, the melting process is evident in images (A) before IR irradiation and (B) after IR irradiation. Without the nanotubes, the images (C) and (D) show no melting.

The picosecond heating of CNTs is followed by a slow recovery (Figure 1C) with a return to the initial temperature (cooling) on a larger time scale. For water at 22 °C, the recovery time is 526 ps whereas for DMF (not shown) it is slower, being at 574 ps. In contrast to the heating time, the recovery time is affected by the initial temperature: it becomes 712 ps for water and 796 ps for DMF, when the initial temperature is raised to 70 °C (Figure 1C). This is consistent with thermodynamic consideration of the temperature difference between the hot tube and the solvent, providing further support of the heat transfer mechanism to the solvent. It follows that heat dissipation from the hot CNTs to surrounding solvents is complete within several hundred picoseconds, depending on solvent thermal conductivity and initial temperature. The heat diffusion, which occurs in the microsecond domain,[11] is unlikely to play a significant role here. Finally, when the IR laser power was increased, microbubbles were observed, indicating that the temperature is high enough to be above the solvent's boiling point (bubble formation). The time constants of cooling can be compared with those characteristic of nanoscale materials, such as gold nanoparticles.[14,15]

Given the metallic/semiconductor nature of the nanotubes, the states excited in the IR/UV processes are complex. To determine that the infrared laser excitation does indeed induce heating, we carried out experiments in our ultrafast electron microscope (UEM-1).[16] Equal amounts of gold spherical nanoparticles (50-nm average diameter) were deposited on two silicon nitride microscope grids with and without MWNTs. Figure 2A−D depicts the observed images of two specimens, before and after the *in situ* laser irradiation under identical conditions (8000 pulses of 120 fs duration and 1.1 nJ energy at 80 MHz; $\lambda = 776$ nm). Such pulses melted the gold nanoparticles in the presence of the MWNTs, but no change was observed when the specimen was irradiated in the absence of MWNTs. Although the wavelength of the fs pulses is shorter than those used in solution, bubble formation has been shown to occur at both wavelengths.[7] The images indicate that the photon energy absorbed by the nanotubes was converted into enough heat to cause the melting of the gold nanoparticles. For the nanoparticles of the size used in this experiment, the absorption band is at ∼515 nm, far from the 776 nm of the excitation; they have a melting point of ∼1300 K.[5] Interestingly, melted nanoparticles could be found as far as 200 μm away from the center of the 100 μm laser spot which suggests significant heat transfer through the substrate.

In conclusion, microscopy imaging indicates that the *in situ* CNTs irradiation with relatively low dosages of infrared radiation results in significant heating of the tubes, which in turn can melt nanoparticles at temperatures above 1300 K. The ultrafast *T*-jump experiments, on the other hand, have revealed, for the first time, that the time scales of CNTs heating and cooling are on the tens and hundreds of picoseconds, respectively. Given the reported transient behavior, these observations suggest novel ways for a *T*-jump methodology, unhindered by the requirement for excitation of water in the study of biological structures.[11,12] They also provide the rate information needed for optimization of photothermal therapy that invokes infrared irradiation to selectively heat and annihilate cancer cells (see ref 17).

In regard to experimental details, the carboxyl functionalization of the CNTs (Sigma-Aldrich, 10-nm average diameter) was synthesized as reported previously.[18] MeOH and DMF were purchased from Sigma-Adrich and used without further purification. The detailed experimental setups for ultrafast laser *T*-jump and UEM-1 have been described before.[11,16]

Acknowledgment. This work was supported by the NSF and Air Force Office of Scientific Research in the Gordon & Betty Moore Physical Biology Center at Caltech. We thank Mr. Akram S. Sadek for his effort in the initial phase of this work.

References

(1) Iijima, S. *Nature* **1991**, *354*, 56.
(2) Kam, N. W. S.; O'Connell, M.; Wisdom, J. A.; Dai, H. J. *Proc. Natl. Acad. Sci. U.S.A.* **2005**, *102*, 11600.
(3) Kostarelos, K.; Lacerda, L.; Pastorin, G.; Wu, W.; Wieckowski, S.; Luangsivilay, J.; Godefroy, S.; Pantarotto, D.; Briand, J. P.; Muller, S.; Prato, M.; Bianco, A. *Nat. Nanotechnol.* **2007**, *2*, 108.
(4) Pop, E.; Mann, D.; Cao, J.; Wang, Q.; Goodson, K.; Dai, H. *Phys. Rev. Lett.* **2005**, *95*, 4.
(5) Begtrup, G. E.; Ray, K. G.; Kessler, B. M.; Yuzvinsky, T. D.; Garcia, H.; Zettl, A. *Phys. Rev. Lett.* **2007**, *99*, 155901.
(6) Izard, N.; Billaud, P.; Riehl, D.; Anglaret, E. *Opt. Lett.* **2005**, *30*, 1509.
(7) Vivien, L.; Riehl, D.; Delouis, J. F.; Delaire, J. A.; Hache, F.; Anglaret, E. *J. Opt. Soc. Am. B* **2002**, *19*, 208.
(8) Riggs, J. E.; Guo, Z. X.; Carroll, D. L.; Sun, Y. P. *J. Am. Chem. Soc.* **2000**, *122*, 5879.
(9) Banerjee, S.; Wong, S. S. *J. Am. Chem. Soc.* **2002**, *124*, 8940.
(10) Luo, Y.; Xia, X.; Liang, Y.; Zhang, Y.; Ren, Q.; Li, J.; Jia, Z.; Tang, Y. *J. Solid State Chem.* **2007**, *180*, 1928.
(11) Ma, H. R.; Wan, C. Z.; Zewail, A. H. *J. Am. Chem. Soc.* **2006**, *128*, 6338.
(12) Mohammed, O. F.; Jas, G. S.; Lin, M. M.; Zewail, A. H. *Angew. Chem., Int. Ed.* **2009**, *48*, 5628.
(13) Hone, J.; Batlogg, B.; Benes, Z.; Johnson, A. T.; Fischer, J. E. *Science* **2000**, *289*, 1730.
(14) Link, S.; Burda, C.; Nikoobakht, B.; El-Sayed, M. A. *J. Phys. Chem. B* **2000**, *104*, 6152.
(15) Kwon, O.-H.; Lee, S.; Jang, D.-J. *Eur. Phys. J. D* **2005**, *34*, 243.
(16) Lobastov, V. A.; Srinivasan, R.; Zewail, A. H. *Proc. Natl. Acad. Sci. U.S.A.* **2005**, *102*, 7069.
(17) Jain, P. K.; Huang, X. H.; El-Sayed, I. H.; El-Sayed, M. A. *Acc. Chem. Res.* **2008**, *41*, 1578.
(18) Liu, Z. F.; Shen, Z. Y.; Zhu, T.; Hou, S. F.; Ying, L. Z.; Shi, Z. J.; Gu, Z. N. *Langmuir* **2000**, *16*, 3569.

JA908079X